Determination of Wetting Behavior, Spread Activation Energy, and Quench Severity of Bioquenchants

K. NARAYAN PRABHU and PETER FERNANDES

An investigation was conducted to study the suitability of vegetable oils such as sunflower, coconut, groundnut, castor, cashewnut shell (CNS), and palm oils as quench media (bioquenchants) for industrial heat treatment by assessing their wetting behavior and severity of quenching. The relaxation of contact angle was sharp during the initial stages, and it became gradual as the system approached equilibrium. The equilibrium contact angle decreased with increase in the temperature of the substrate and decrease in the viscosity of the quench medium. A comparison of the relaxation of the contact angle at various temperatures indicated the significant difference in spreading of oils having varying viscosity. The spread activation energy was determined using the Arrhenius type of equation. Oils with higher viscosity resulted in lower cooling rates. The quench severity of various oil media was determined by estimating heat-transfer coefficients using the lumped capacitance method. Activation energy for spreading determined using the wetting behavior of oils at various temperatures was in good agreement with the severity of quenching assessed by cooling curve analysis. A high quench severity is associated with oils having low spread activation energy.

DOI: 10.1007/s11663-007-9060-3

I. INTRODUCTION

WETTABILITY can be defined as the tendency of a liquid to spread on a solid substrate. The contact angle is widely used to measure the wettability of liquid on a solid surface. It is an important parameter in surface science. Contact angle measurements provide a simple and reliable technique for interpretation of surface energies.[1,2,3] The spreading of a liquid drop on a solid can be studied with the knowledge of contact angle measurement and material properties.[4,5,6] The spreading of a liquid drop on a horizontal solid surface can be divided into high speed impact spreading, which is inertia dominated or forced spreading and low speed impact spreading dominated by surface tension. Spontaneous spreading occurs when the impact speed is equal to zero.[7] Gu *et al*. developed a model to study the spreading process of liquid drop on the solid surface.[8] The spreading model accounts for the inertial, viscous, and gravitational forces; the interfacial tensions; and the contact angle of the solid-liquid-fluid system. The model could predict the spontaneous spreading of a liquid drop on a solid surface.

Wettability can be characterized by the degree and the rate of wetting.[9,10] The degree of wetting indicates the extent to which the liquid wets the surface and is generally quantified in terms of contact angle formed at the three-phase interface. As a droplet impinges on a solid surface, it spreads under the influence of the inertial and gravitational forces. The restraining forces are due to wall shear stress and surface tension. The surface tension forces are influenced by the contact angle between the liquid and solid surfaces.[11] Under equilibrium conditions, it is dependent on the surface and interfacial energies involved at the solid/liquid interface. Interfacial phenomena in the three-phase contact line region, where the liquid vapor interface intersects a solid surface, are important for many equilibrium and nonequilibrium phenomena such as contact angle, adsorption, spreading, evaporation boiling, wetting, *etc*.[12] The rate of wetting indicates how fast the liquid spreads on the surface. It is influenced by a number of parameters such as surface texture, temperature of the liquid medium, and substrate and intrinsic properties of the liquid medium. The spreading process is a temperature-dependent and thermally activated process and is influenced by activation energy.[13] The angle formed during the spreading of the liquid drop on the solid surface is called the dynamic contact angle. The drop will become thinner with the increase of the contact radius of the drop and decrease in the height at the center. As a result, the contact angle decreases with spreading as the radius of the drop increases.[14] As the drop spreads, the contact angle θ relaxes from its initial maximum value of 180 deg at the point of contact to its equilibrium angle in the case of partial wetting or zero if the liquid wets the solid completely.[15]

Equilibrium contact angles are functions of surface free energies of the solid substrate and the liquid in contact with it. The equilibrium contact angle depends on the liquid, vapor, material of the surface, surface roughness, and surface impurities. The spreading process will continue until equilibrium is achieved.[16] This equilibrium contact angle represents the extent to which the liquid

K. NARAYAN PRABHU, Assistant Professor, and PETER FERNANDES, Research Scholar, are with the Department of Metallurgical & Materials Engineering, National Institute of Technology Karnataka, Surathkal, Mangalore 575 025, India. Contact e-mail: prabhukn_2002@yahoo.co.in

Manuscript submitted December 23, 2006.
Article published online June 26, 2007.

spreads over the substrate. The basic mathematical treatment of wetting of a solid surface by a liquid is given by the Young–Dupre equation (Eq. [1]), which assumes equilibrium of interfacial energies. A drop of a liquid put on a solid will modify its shape until the equilibrium is attained. Figure 1 is a schematic sketch of a sessile drop of liquid resting on a solid surface. The balance of interfacial energies under equilibrium yields an expression for contact angle (θ) formed at the three-phase contact point given by

$$\cos\theta = (\gamma_{sv} - \gamma_{sl})/\gamma_{lv} \qquad [1]$$

Here, γ represents surface energy and the subscripts s, l, and v indicate solid, liquid, and vapor phases, respectively. An angle of 180 deg indicates zero adhesion between the liquid and surface and therefore represents a total nonwetting condition. For practical purposes, the liquid is said to wet the surface of solid when the contact angle is less than 90 deg. On the other hand, if the contact angle is greater than 90 deg, the liquid is considered as nonwetting. In such cases, the liquid drop tends to move about easily on the substrate surface and does not have any tendency to enter into pores or holes by capillary action. The spreading of industrial oils with various viscosity and surface tension values over the surface of steel substrates has been investigated by Cherednichenko *et al.*[16] The variation of the radius r of the spreading spot followed the power law relationship of the type $A = kt^n$, where k is a proportionality factor, t is the time, and $n = 0.2$. The surface tension and the viscosity of the spreading oil were recommended for characterizing the spreading ability of oils.

Quenching consists of raising the temperature of steel above a certain critical temperature called austenitizing temperature usually in the range of 850 °C to 870 °C and holding it at that temperature for a fixed time and then rapidly cooling in a suitable quench medium to room temperature. Quenching is done to prevent ferrite or pearlite formation and to allow the formation of bainite or martensite. Quenching of steel in liquid medium consists of three distinct stages of cooling: the vapor blanket stage, nucleate boiling stage, and convective stage. In the first stage, a vapor blanket is formed immediately upon quenching. This blanket has an insulating effect, and heat transfer in this stage is slow because it is mostly through radiation. As the temperature drops, the vapor blanket becomes unstable and collapses, initiating the nucleate boiling stage. Heat removal is the fastest in this stage, due to the heat of vaporization, and continues until the surface temperature drops below the boiling point of the quenching medium. Further cooling takes place mostly through convection and some conduction.[17] The resulting properties from quenching depend on cooling rate, quenchant, and thermophysical properties of steel. The effectiveness of quenching depends on the cooling characteristics of the quenching medium as related to the ability of steel to harden.[18] The information on the selection and use of oil, water, salt, aqueous polymers, brine, fluidized bed, and high-pressure gas quenching are discussed in detail by Totten *et al.*[19] Quench severity refers to the ability of a quenchant or a quenching system to extract heat from a sample during quenching. The function of a quench medium is to enhance heat-transfer rates from the hot metal during the quenching process. The rate of heat transfer is influenced by the ability of liquid to wet the surface of the component during quenching. Tensi and Lainer[20] studied rewetting and heat transfer during immersion quenching of high-speed quenching oils. The wettability of a surface was quantified by measuring "wetting" times.

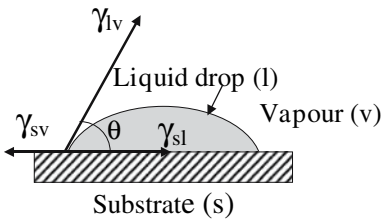

Fig. 1—Schematic sketch showing the evolution of the contact angle (θ) at a solid/liquid interface.

With the increase in awareness and importance attached to environmental issues such as global warming, more environmentally friendly quench media are developed as alternatives to mineral oil. The use of soybean oil as a quench medium was studied in Reference 21. Vegetable oils have poor oxidative properties and their performance as a quench medium can be enhanced by using suitable antioxidants.[22] A bioquenchant can be defined as a renewable quench medium derived from vegetable sources such as sunflower, coconut, palm, and groundnut. Vegetable oils are abundantly available and are cheaper than mineral oil. They are biodegradable and eliminate harmful emissions. An investigation was conducted in the present work to determine the wetting behaviour and severity of quenching of vegetable oil quench media.

II. EXPERIMENT

For wetting studies, the experimental setup consisted of a dynamic contact angle analyzer (FTA 200). The equipment is capable of capturing and analyzing the spreading process of a liquid on a solid substrate. The equipment has a flexible video system for measuring the contact angle, surface, and interfacial energies. A droplet of test liquid was dispensed using a surgical syringe with a precision flow control valve onto the steel substrate, and the spreading phenomenon was recorded at 60 images per second. Captured images were analyzed using FTA image analysis software to determine the contact angle. The measurement errors associated with the contact angle measurement are attributed to the electronic noise in the image and the baseline uncertainty. In the FTA instrument, the error associated per pixel is about 0.5 deg. The baseline could be set manually to minimize this error. The experiments were repeated to ensure the consistency of the test results. The

analysis of variance (ANOVA) method was used to compare the experimental data sets. The statistical results were interpreted by evaluating the F ratio. If the F value is greater than F_{crit}, then there is a statistically significant difference. For example, with cashewnut shell (CNS) liquid, the calculated values of F and F_{crit} were found to be 0.083 and 6.7, respectively, at 99 pct confidence level. Hence, it was concluded that the differences in the contact angles obtained with two experimental trials were not statistically significant. Similar results were obtained with other oils as well.

The temperature of the substrate was maintained at 30 °C, 50 °C, 75 °C, 100 °C, 125 °C, 150 °C, and 175 °C in a temperature-controlled environment chamber. The surface of the substrate was prepared by using different grades of emery papers to attain a mean surface roughness (R_a) of 0.75 ± 0.02 μm. R_a is the arithmetic mean of the absolute value of the profile departures from the centerline within the evaluation length. The surface roughness (R_a) was measured using a surface roughness tester (Mitutoyo Surftest-211). Mineral oil (SN 150) and six commercially available vegetable oils, namely, sunflower, coconut, palm, groundnut, castor, and CNS oil, were used as test liquids for wetting studies on stainless steel (type 304) substrate. Table I gives the typical fatty acid composition of vegetable oils.

For assessment of quench severity, the experimental setup consisted of a vertical tubular electric resistance furnace open at both ends. A beaker containing 2000 mL of quenchant was placed directly underneath the furnace so that the heated probe could be transferred quickly to the quenching medium. Quench probe was prepared from type 304 stainless steel for assessment of quench severity. The probe was instrumented with a calibrated K-type thermocouple of 0.45-mm diameter enclosed in a ceramic sheath of 3-mm diameter. The thermocouple was inserted in a hole of diameter 3 mm drilled on the top surface of the probe and care was taken to ensure tight fit and good contact condition. The thermocouple junction was exposed and is in direct contact with the probe for quick response. The time constant of the thermocouple used was found to be 0.4 seconds in water medium. The other end of the thermocouple was connected to a PC-based temperature data acquisition system (NI SCXI 1000) *via* a compensating cable. The dimensions of the probe and the location of the thermocouple are given in Figure 2. The probe was heated to 850 °C in an electric resistance furnace and was quickly transferred to a beaker containing 2000 mL of quench medium. The ratio of the mass of quench medium to the stainless steel probe was about 33 for all the experiments.

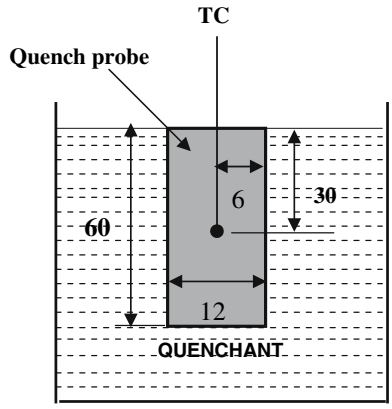

Fig. 2—Schematic sketch of the quench probe immersed in the quench medium.

III. RESULTS AND DISCUSSION

A. *Effect of Temperature on Wetting Behavior*

Figure 3 shows the photographic images of relaxation of coconut oil droplet on a stainless steel substrate at different temperatures. High contact angles were observed during initial stages of the relaxation for all oil media. The relaxation of the contact angle was sharp during the initial stages, and it became gradual as the system approached equilibrium. The contact angle decreases with increase in temperature of the substrate. Figure 4 shows the typical contact angle relaxation curve of oil medium on a stainless steel substrate at various temperatures. Figure 5 shows the effect of temperature on equilibrium contact angles of oil media. It clearly shows that the equilibrium contact angle decreases with the increase in the temperature of the substrate. In the present study, the equilibrium contact angle (θ) was defined as the contact angle during relaxation of liquid media beyond which $d\theta/dt$ is ≤0.01 deg/ms. A higher equilibrium contact angle was obtained for castor oil (36 deg), and a lower equilibrium contact angle was obtained for sunflower oil (19 deg) on a stainless steel substrate at 30 °C. Palm oil shows the

Table I. Fatty Acid Composition of Bioquenchants

	Type of Fatty Acids, Wt Pct		
Bioquenchant	Saturated	Monounsaturated	Polyunsaturated
Sunflower oil	12	19	69
Coconut oil	92	6	2
Palm oil	50	40	10
Groundnut oil	20	54	26
Castor oil	3	91	6
CNS oil	25	58	17

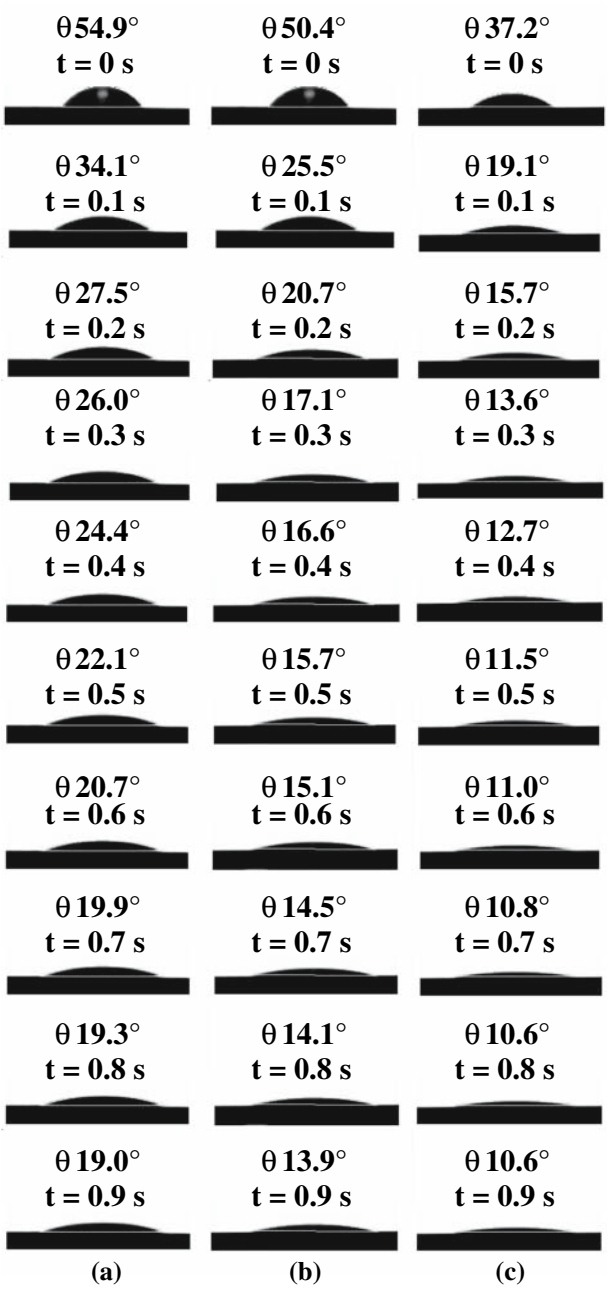

Fig. 3—Typical images showing the relaxation of contact angle at (*a*) 30 °C, (*b*) 75 °C, and (*c*) 175 °C. Quench medium: coconut oil.

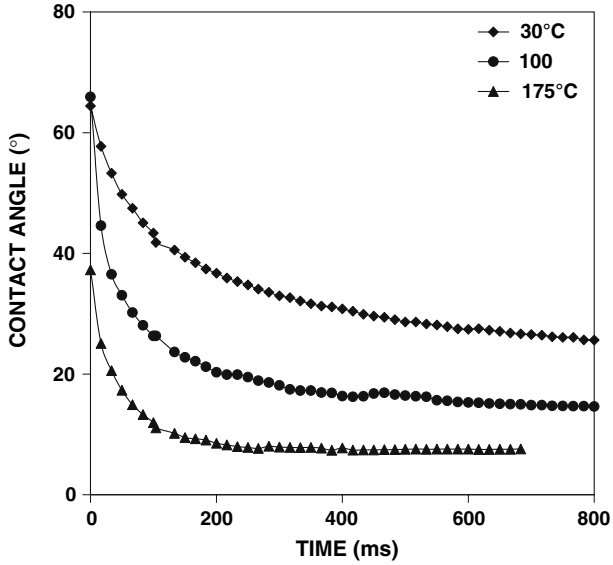

Fig. 4—Effect of temperature on relaxation of contact angle of sunflower oil.

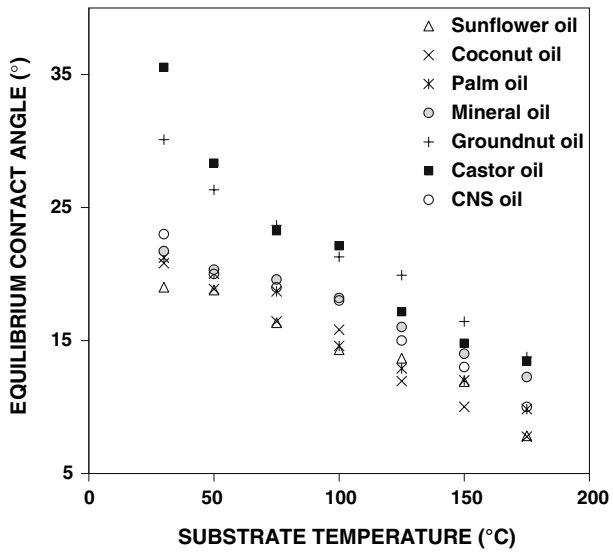

Fig. 5—Effect of temperature on equilibrium contact angle of different oil media.

intermediate equilibrium contact angle value (21 deg). Equilibrium contact angles decreased to 13, 8, and 10 deg for castor, sunflower, and palm oils on a stainless steel substrate at 175 °C, respectively. Figure 6 shows the temperature dependency of spreading of liquid media. The time required to reach the equilibrium state decreased with the increase in temperature. The relaxation time to reach the equilibrium state was higher for castor oil (1433 ms at 30 °C) and lowest for sunflower oil (866 ms at 30 °C). The relaxation time decreases with the increase in temperature of the substrate.

Figure 7 shows the plot of ln (spread radius) *vs* ln (time) for palm oil. It consists of three regimes, namely, capillary, gravity, and viscous. At higher temperature (175 °C), palm oil spreading was almost terminated and is indicated by the viscous regime. However, at a lower temperature (30 °C), the spreading was still in the gravity regime with nearly a constant slope. This indicates that the spreading of the oil has not been terminated. Figures 8 through 10 show corresponding plots for coconut, mineral, CNS, and castor oils during spreading on stainless steel substrate at 30 °C, 100 °C, and 175 °C, respectively. The spreading behavior of different oils on stainless steel substrate at various temperatures consisted of an initial capillary regime followed by gravity and viscous regimes. Significant spreading was observed in all liquid media at higher temperatures. The higher spread area is the indication of

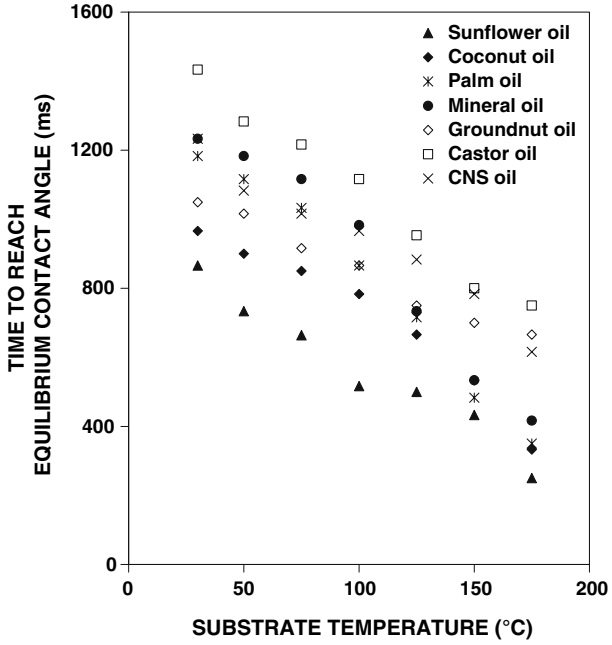

Fig. 6—Temperature dependency of spreading of different oil media.

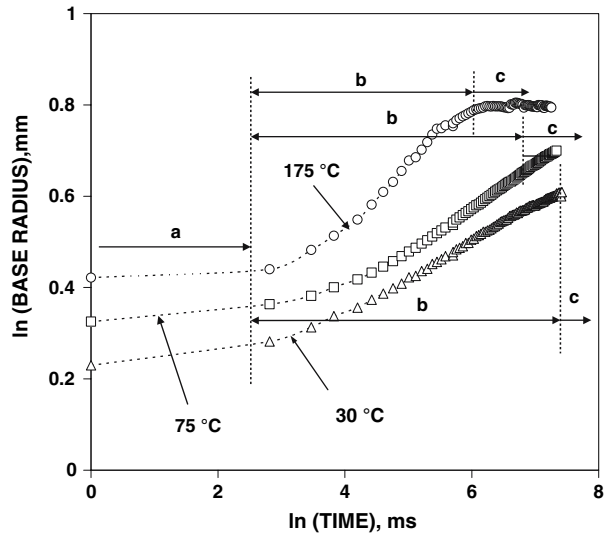

Fig. 7—Rate of spreading of palm oil at 30 °C showing (*a*) capillary, (*b*) gravity, and (*c*) viscous regimes.

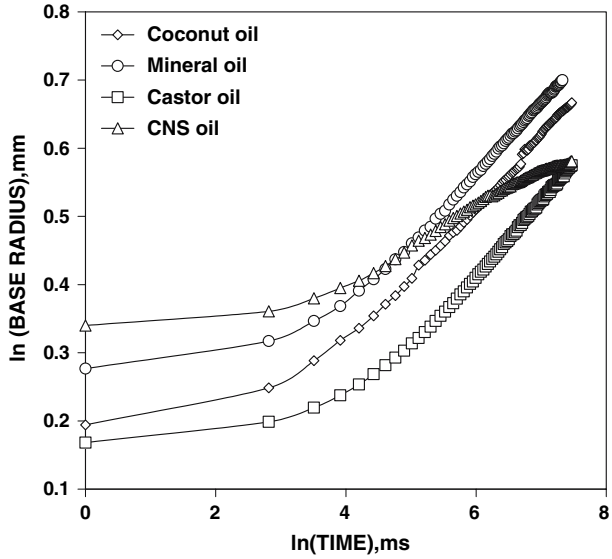

Fig. 8—Rate of spreading of different oils at 30 °C showing various regimes.

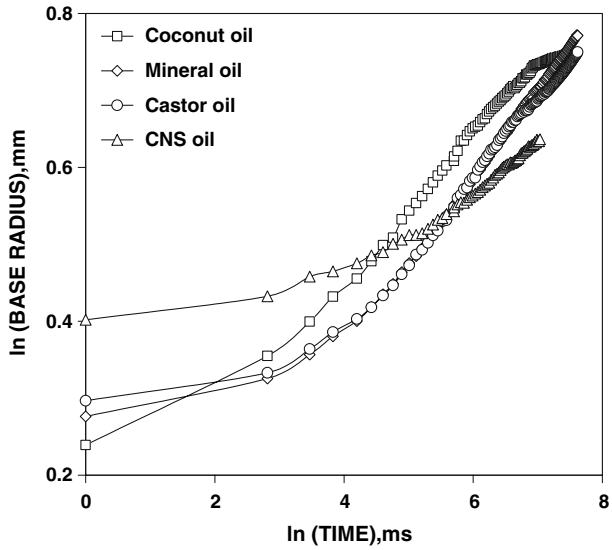

Fig. 9—Rate of spreading of different oils at 100 °C showing various regimes.

the spreading of liquid drop during relaxation resulting in a lower contact angle. The oil started spreading rapidly with a relatively high velocity resulting in a sharp increase of base area during early stages of spreading. However, within a very short period, the spreading rate significantly reduced to almost zero, indicating the stabilization condition. This is due to the attainment of equilibrium between the various surface forces under action. The further relaxation of contact angle, increase of spread area, and variation in velocity were found to be negligible. Viscous forces dominated the spreading of oil at lower temperatures. Hence, during spreading of oil at lower temperatures, longer periods of time are generally required to achieve equilibrium. Spreading was almost terminated in the viscous regime at higher temperature (175 °C) for all oil media except CNS oil. This was indicated by the negligible change in the base radius due to viscous forces. However, spreading of CNS oil was still in the gravity regime (at 175 °C), indicating that spreading has not been terminated. At 30 °C, spreading was in the gravity regime for all oil media, whereas at 100 °C, spreading was terminated in the viscous regime for all oil media except castor and CNS oils. The CNS oil exhibited a unique spreading behavior. During spreading of CNS oil, longer periods of time are required to achieve equilibrium. A comparison of the relaxation of

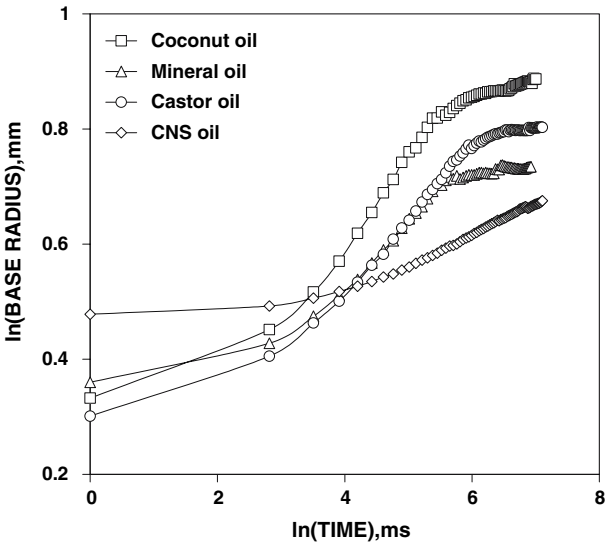

Fig. 10—Rate of spreading of different oils at 175 °C showing various regimes.

contact angle at various temperatures indicated the significant difference in the spreading behavior between lower viscosity sunflower oil with highly viscous castor oil. Mineral oil (SN150), a conventional quench medium, exhibited the intermediate spreading behavior. The variation of kinematic viscosity of different oils at various temperatures is shown in Figure 11. The lowest kinematic viscosity of 0.3975×10^{-4} m^2/s was obtained for coconut oil, and the highest kinematic viscosity of 4.88×10^{-4} m^2/s was obtained for castor oil at 30 °C. Viscosity of oils decreases with the increase in temperature. All of the oils have nearly equal densities (0.9 ± 0.02 g/cc), and almost equal quantities of oil drops were dispensed during experiments. Therefore, the gravity effect during spreading should be identical. However, the viscosity values for these oils are significantly different. Coconut and sunflower oils have low viscosities and therefore spread faster. On the other hand, viscosity of castor oil is high and resulting in a slow spreading on a substrate. The spreading rate increased due to the increase in temperature of the substrate. This is due to the fact that the increase in temperature reduces both the viscosity of liquid media and the surface energy, resulting in enhanced spreading. Among oils, lower viscosity oils such as sunflower and coconut oils show the higher base radius as compared to higher viscosity castor oil. Oils having higher viscosity offer greater resistance to flow during spreading as compared to lower viscosity oils, resulting in a higher equilibrium contact angle.

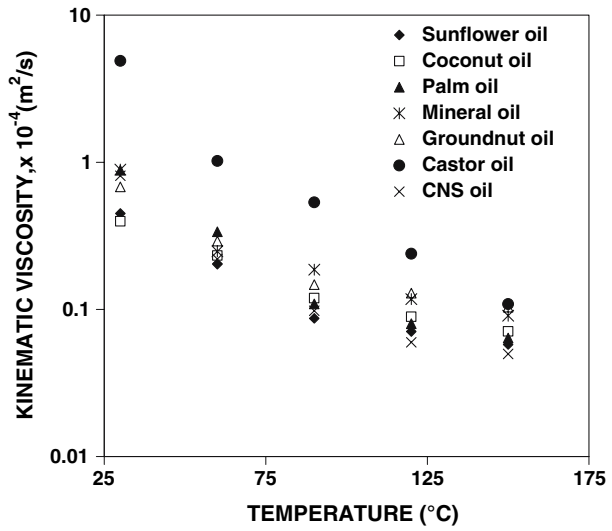

Fig. 11—Variation of viscosity of different oils with temperature.

B. *Determination of Activation Energy for Spreading*

The relaxation of contact angle was very fast and the initial droplet images could not be recorded. It was assumed that at time $t = 0$, the contact angle is 180 deg for all the oils. However, during experiments, the actual contact angle values obtained initially were significantly lower than 180 deg due to the rapid spreading of the droplets immediately on contact with the substrate. Lower initial contact angles were obtained with oils having lower viscosity. For all of the vegetable oil experiments, the time required to reach 20 deg was measured and the rate of contact angle relaxation was computed for temperatures varying from 30 °C to 175 °C. Figures 12 and 13 show the variation of contact angle relaxation rate with the reciprocal of absolute temperature for various oil media. The rate of relaxation of contact angle rate was maximum at higher temperatures.

The variation of rate of contact angle relaxation with temperature could be described by an Arrhenius type of equation as

$$\frac{\Delta\theta}{\Delta t} = A \exp\left(\frac{-E_a}{RT}\right) \qquad [2]$$

where

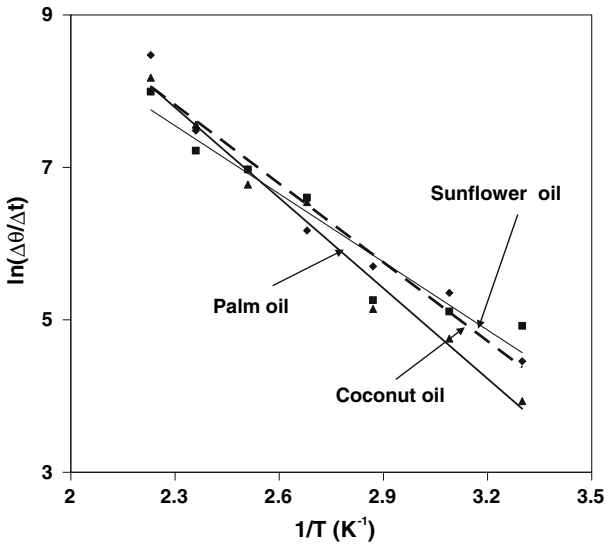

Fig. 12—Arrhenius plot of spreading of sunflower, coconut, and palm oils.

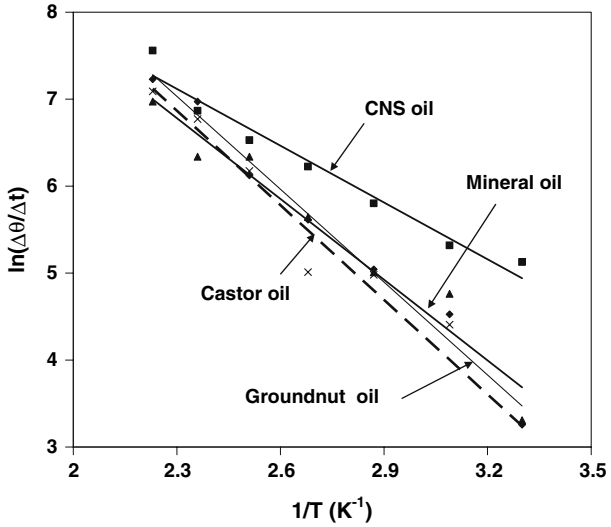

Fig. 13—Arrhenius plot of spreading of mineral, groundnut, castor, and CNS oils.

$\Delta\theta/\Delta t$ = rate of contact angle relaxation,
E_a = activation energy of the liquid (J/mol),
R = the gas constant (8.314 J/mol K), and
T = the absolute temperature (K).

Equation [2] is rewritten as

$$\ln\frac{\Delta\theta}{\Delta t} = \ln A + \left(\frac{-E_a}{\mathrm{R}T}\right) \qquad [3]$$

A plot of ln $(\Delta\theta/\Delta t)$ *vs* $1/T$ is a straight line of the type

$$y = mx + b$$

where

$$x = 1/T,$$

$$y = \ln(\Delta\theta/\Delta t),$$

$$b = \ln A, \text{ and}$$

$$m = -E_a/\mathrm{R}.$$

From the slopes of straight lines (Figures 12 and 13), the activation energy for relaxation is computed. An increase in temperature increases the relaxation rate. Higher values of activation energy indicate a greater temperature dependency of contact angle relaxation. The estimated activation energies for relaxation for various vegetable oils along with conventional mineral oil are given in Table II. Castor oil shows the maximum activation energy of 24.9 kJ/ mole compared to other oils. The sunflower oil has the lowest activation energy of 16.9 kJ/ mole. Activation energy plays an important role in spreading phenomenon of oil media. More spreading was observed in sunflower oil having lower activation energy as compared to castor oil with higher activation energy. Spreading of sunflower oil was terminated early as compared to castor oil. The low spread activation energy of sunflower oils makes it spread faster than other oils on the stainless steel substrate. Castor oil showed poor spreading due to its higher activation energy. The spread activation energy was found to be influenced by the fatty acid composition of oils. Oils having a higher percentage of monounsaturated fatty acids generally showed higher spread activation energy and lower degree of spreading.

Table II. Estimated Spread Activation Energies of Various Oil Quenchants

Medium	Activation Energy (J/mole)
Sunflower oil	16,960
Coconut oil	17,243
Palm oil	18,149
Mineral oil	18,506
Groundnut oil	24,409
Castor oil	24,950
CNS oil	18,906

C. *Assessment of Severity of Quenching*

Heat-transfer characteristics of vegetable oils along with the conventional mineral oil were determined during lateral quenching of stainless steel (type 304) probe. Figure 14 shows the typical cooling curve of the stainless steel probe subjected to lateral quenching. Cooling rate parameters during immersion quenching of stainless steel probe in different oil media are given in Table III. A highest peak cooling rate of 42 °C/s was obtained for both sunflower and coconut oils at 661 °C and 663 °C, whereas castor oil shows the lowest peak cooling rate of about 29 °C/s at 747 °C during quenching.

Time-varying heat-transfer coefficients were calculated from the experimentally measured cooling curves

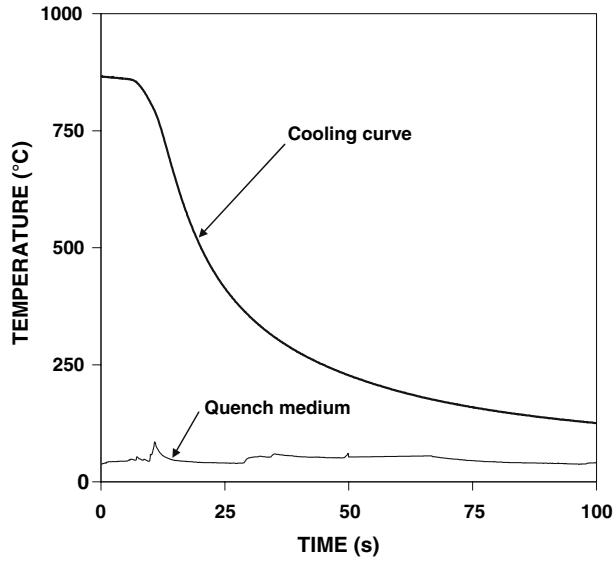

Fig. 14—Typical thermal history during immersion quenching.

Table III. Measured Cooling Rate (CR) Parameters during Immersion Quenching of Stainless Steel Probe in Various Oil Media

Quench Media	Peak CR (°C/s)	Temperature at Maximum CR (°C)	CR at 600 °C (°C/s)	CR at 500 °C (°C/s)	CR at 400 °C (°C/s)	CR at 300 °C (°C/s)
Sunflower oil	42	661	35	29	12	6
Coconut oil	42	663	35	23	12	6
Palm oil	41	662	35	28	13	7
Mineral oil (SN150)	38	750	28	18	12	6
Groundnut oil	35	735	29	23	12	6
Castor oil	29	747	28	23	12	6
CNS oil	35	741	29	23	12	6

by assuming Newtonian cooling (Bi $= hL_c/k < 0.1$) of the probe. Bi is the Biot number, L_c is the characteristic length (V/A) of the probe, and k is the thermal conductivity of the probe material (type 304 stainless steel). If the temperature of the probe is uniform during the cooling process (Bi < 0.1), the heat loss from the probe Q is equal to the decrease in internal energy of the probe. Thus,

$$Q = hA(T_p - T_q) = -C_p \rho V \left(\frac{dT_p}{dt}\right) \quad [4]$$

where

Q = the heat flow rate, W;
h = heat-transfer coefficient on the probe surface, W/m^2 K;
A = surface area of the probe, m^2;
T_p = temperature of the probe, K;
T_q = temperature of the quench medium, K;
C_p = specific heat of the probe material, J/kg K;
ρ = specific density of the probe material, kg/m^3;
V = volume of the probe, m^3;
t = time, s; and
(dT_p/dt) = cooling rate of the probe, K/s.

The quenchant temperature (T_q) around the probe is assumed to be uniform and the preceding equation is rearranged as

$$q = h(T_p - T_q) = -C_p \rho \frac{V}{A} \left(\frac{dT_p}{dt}\right) \quad [5]$$

The heat-transfer coefficient (h) can be calculated from the cooling rate (dT_p/dt) using the equation

$$h = C_p \rho \frac{V}{A} \left(\frac{dT_p/dt}{(T_p - T_q)}\right) \quad [6]$$

Equation [6] shows that the preciseness of the heat-transfer coefficient estimated depends on the accuracy of the cooling rate obtained from the cooling curve data. In the present work, experiments were repeated at least twice and the ANOVA technique was adopted to compare the cooling curves obtained with the same quench medium. The experimental data sets between which there was no statistically significant difference were used in the lumped capacitance model to assess heat-transfer coefficients.

To determine the effect of the presence of thermocouple on the measured thermal history, heat-transfer simulation was carried out for the probe with and without the alumina thermocouple sheath having a diameter of 3 mm. A one-dimensional Fourier heat conduction equation was solved directly with boundary heat-transfer coefficients of 800 and 400 W/m^2 K. The thermal histories obtained with and without the thermocouple are compared. At a heat-transfer coefficient of 800 W/m^2 K, the variation between the thermal histories was less than 2 pct at all temperatures. At the lower boundary heat-transfer coefficient of 400 W/m^2 K, there was no significant variation between the thermal histories, and the variation was below 1 pct. The contact resistance between the thermocouple sheath and the stainless steel probe was assumed to be negligible in the simulation. Figure 15 shows the thermal histories at the geometric center of the probe computed for a boundary heat-transfer coefficient of 800 W/m^2 K with and without the thermocouple.

Figures 16 and 17 show the variation of heat-transfer coefficients (h) with time during lateral quenching of stainless steel probe in different oil media. Sunflower oil shows the maximum peak heat-transfer coefficient (755 W/m^2 K), and castor oil shows the minimum peak heat-transfer coefficient (630 W/m^2 K). The peak heat-transfer coefficients obtained with palm oil (713 W/m^2 K) were comparable to mineral oil (698 W/m^2 K), a conventional quench medium. The cooling rate and heat-transfer

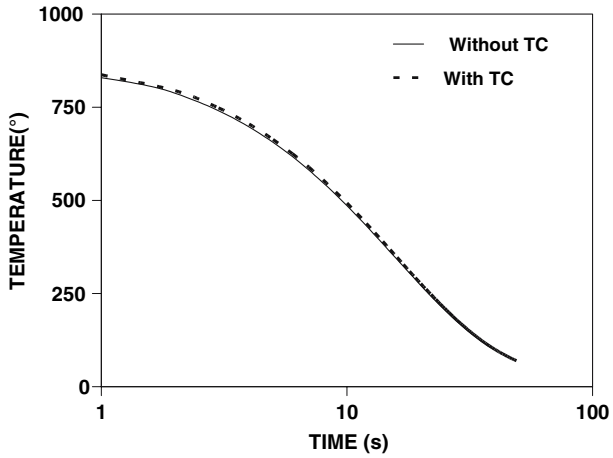

Fig. 15—Effect of the presence of thermocouple on thermal history at the geometric centre of the probe.

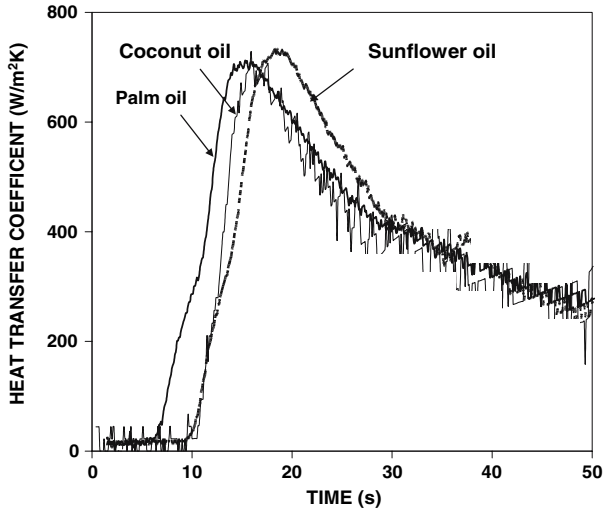

Fig. 16—Heat-transfer coefficients for sunflower, coconut, and palm oils.

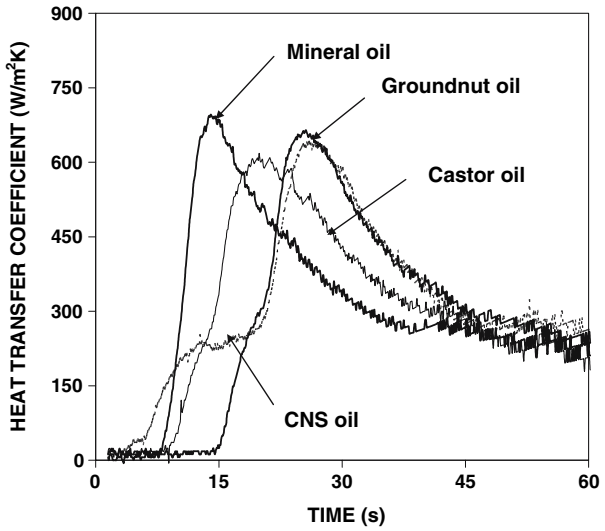

Fig. 17—Heat-transfer coefficients for groundnut, mineral, castor, and CNS oils.

coefficients were found to be strongly dependent on the viscosity of quench medium. A lower heat-transfer rate was observed with higher viscosity oils. Higher viscosity castor oil shows the lowest rate of heat transfer as compared to other oil media, whereas low viscosity sunflower and coconut oils show high rates of heat transfer.

Spread activation energies determined using the wetting behavior of oils at various temperatures were in good agreement with quench severities assessed by cooling curve analysis. Based on the quench severity and activation energy, the effectiveness of quenching of oil media could be arranged in the following order.

Sunflower oil > Coconut oil > Palm oil > Mineral oil > CNS oil > Groundnut oil > Castor oil

Lower heat-transfer coefficients were obtained for castor oil due to its poor rate of spreading. A high quench severity is associated with oils having low spread activation energy. Palm and CNS oil could be used as effective bioquenchants for industrial heat treatment. The CNS oil is cheaper compared to the other vegetable oils. However, palm oil has superior oxidation strength, as indicated by its lower total acidity number (TAN). The TAN value of palm oil (1.28 mg of KOH/g) is significantly lower than CNS oil (86.5 mg of KOH/g) and mineral oil (2.3 mg of KOH/g).

IV. CONCLUSIONS

The severity of the quenching and wetting behaviors of bioquenchants were assessed in the present work to study the suitability of vegetable oils for industrial heat treatment. Based on the results of the investigation, the following conclusions were drawn.

1. Equilibrium contact angle of quench media decreases with increase in the temperature of the substrate. During spreading of oil at lower temperatures, longer periods of time are generally required to achieve equilibrium. The time to reach the equilibrium state decreases with an increase in temperature.
2. Lower viscosity oils show better spreading and improved wettability on the stainless steel substrate as compared to viscous oils.
3. The temperature-dependent contact angle data were used to determine the spread activation energy of quench media. The activation energy for spreading was maximum for sunflower oil and minimum for viscous castor oil.
4. The spread activation energies determined using the wetting behavior of oils at various temperatures were in good agreement with the severities of quenching assessed by cooling curve analysis. A high quench severity is associated with oils having low spread activation energy.

REFERENCES

1. C.N.C. Lam, N. Kim, D. Hui, D.Y. Kwok, M.L. Hair, and A.W. Neumann: *Coll. Surf. A*, 2001, vol. 189, pp. 265–78.
2. D.N. Rao: *Coll. Surf. A*, 2003, vol. 206, pp. 203–16.
3. A. Perwuelz, T.N. De Olivera, and C. Caze: *Coll. Surf. A*, 1999, vol. 147, pp. 317–29.
4. M. Brugnara, E. Degasperi, C. DellaVolpe, D. Maniglio, A. Penati, S. Siboni, L. Toniolo, T. Poli, S. Invernizzi, and V. Castelvetro: *Coll. Surf. A*, 2004, vol. 241, pp. 299–312.
5. J. Eggers and R. Evans: *J. Coll. Interface Sci.*, 2004, vol. 280, pp. 537–38.
6. D. Erickson, B. Blackmore, and D. Li: *Coll. Surf. A*, 2001, vol. 182, pp. 109–22.
7. B.B. Sauer and W.G. Kampert: *J. Coll. Interface Sci.*, 1998, vol. 199, pp. 28–37.
8. Y. Gu and D. Li: *Coll. Surf. A*, 1998, vol. 142, pp. 243–56.
9. P.T. Vianco and D.R. Frear: *JOM*, 1993, vol. 45, pp. 14–19.
10. D.R. Frear, W.B. Jones, and K.R. Kinsman: *Solder Mechanics—A State of the Art Assessment*, TMS, Warrendale, PA, 1991, pp. 1–106.

11. S.G. Kandlikar and M.E. Steinke: *Int. J. Heat Mass Trans.*, 2002, vol. 45, pp. 3771–80.
12. S.J. Gokhale, J.L. Plawsky, and P.C. Wayner, Jr.: *J. Coll. Interface Sci.*, 2003, vol. 259, pp. 354–66.
13. V.H. Lopez and A.R. Kennedy: *J. Coll. Interface Sci.*, 2006, vol. 298, pp. 356–62.
14. A. Amirfazli, D. Chatain, and A.W. Neumann: *Coll. Surf. A*, 1998, vol. 142, pp. 183–88.
15. J. De Coninck, M.J. de Ruijter, and M. Voue: *Curr. Opin. Coll. Interface Sci.*, 2001, vol. 6, pp. 49–53.
16. G.I. Cherednichenko, M.A. Al'tshuler, N.A. Terent'eva, and V.P. Temnenko: *Coll. J. USSR*, 1984, vol. 46, pp. 162–64.
17. C. Tszeng and P. Nash: *Indust. Heat.*, 2001, vol. 68, pp. 12–14.
18. A.J. Fletcher and W.D. Griffiths: *Mater. Sci. Technol.*, 1993, vol. 9, pp. 176–82.
19. G.E. Totten, C.E. Bates, and N.A. Clinton: *Handbook of Quenching and Quenching Technology*, ASM INTERNATIONAL, Materials Park, OH, 1993.
20. H.M. Tensi and K. Lainer: *Harterei-Technische Mitteilungen (Germany)*, 1997, vol. 52, pp. 298–303.
21. L.C.F. de Canale, M.R. Fernandes, S.C.M. Agustinho, G.E. Totten, and A.F. Farah: *Int. J. Mater. Product Technol.*, 2005, vol. 24, pp. 101–25.
22. K. Lainer, H.M. Tensi, and G.E. Totten: *In 18th Heat Treating Society Conf. Proc.*, H. Walton and R. Wallis, eds., ASM International, Materials Park, OH, 1998, pp. 568–74.